# *EML4-ALK* Fusion Gene and Efficacy of an ALK Kinase Inhibitor in Lung Cancer

Jussi P. Koivunen,[1,2] Craig Mermel,[2,9] Kreshnik Zejnullahu,[1,2] Carly Murphy,[4] Eugene Lifshits,[6] Alison J. Holmes,[1,2] Hwan Geun Choi,[3,7] Jhingook Kim,[10,11] Derek Chiang,[2,9] Roman Thomas,[12] Jinseon Lee,[10,11] William G. Richards,[8] David J. Sugarbaker,[8] Christopher Ducko,[8] Neal Lindeman,[4] J. Paul Marcoux,[1,2,4] Jeffrey A. Engelman,[6] Nathanael S. Gray,[3,7] Charles Lee,[4] Matthew Meyerson,[1,2,3,4] and Pasi A. Jänne[1,2,5]

**Abstract**

**Purpose:** The *EML4-ALK* fusion gene has been detected in ∼7% of Japanese non-small cell lung cancers (NSCLC). We determined the frequency of *EML4-ALK* in Caucasian NSCLC and in NSCLC cell lines. We also determined whether TAE684, a specific ALK kinase inhibitor, would inhibit the growth of *EML4-ALK*-containing cell lines *in vitro* and *in vivo*.

**Experimental Design:** We screened 305 primary NSCLC [both U.S. ($n = 138$) and Korean ($n = 167$) patients] and 83 NSCLC cell lines using reverse transcription-PCR and by exon array analyses. We evaluated the efficacy of TAE684 against NSCLC cell lines *in vitro* and *in vivo*.

**Results:** We detected four different variants, including two novel variants, of *EML4-ALK* using reverse transcription-PCR in 8 of 305 tumors (3%) and 3 of 83 (3.6%) NSCLC cell lines. All *EML4-ALK*-containing tumors and cell lines were adenocarcinomas. *EML4-ALK* was detected more frequently in NSCLC patients who were never or light (<10 pack-years) cigarette smokers compared with current/former smokers (6% versus 1%; $P = 0.049$). TAE684 inhibited the growth of one of three (H3122) *EML4-ALK*-containing cell lines *in vitro* and *in vivo*, inhibited Akt phosphorylation, and caused apoptosis. In another *EML4-ALK* cell line, DFCI032, TAE684 was ineffective due to coactivation of epidermal growth factor receptor and ERBB2. The combination of TAE684 and CL-387,785 (epidermal growth factor receptor/ERBB2 kinase inhibitor) inhibited growth and Akt phosphorylation and led to apoptosis in the DFCI032 cell line.

**Conclusions:** *EML4-ALK* is found in the minority of NSCLC. ALK kinase inhibitors alone or in combination may nevertheless be clinically effective treatments for NSCLC patients whose tumors contain *EML4-ALK*.

**Authors' Affiliations:** [1]Lowe Center for Thoracic Oncology and Departments of [2]Medical Oncology and [3]Cancer Biology, Dana-Farber Cancer Institute; Departments of [4]Pathology and [5]Medicine, Brigham and Women's Hospital and Harvard Medical School; [6]Massachusetts General Hospital Cancer Center; [7]Department of Biological Chemistry and Molecular Pharmacology, Harvard Medical School; [8]Department of Surgery, Brigham and Women's Hospital, Boston, Massachusetts; [9]The Broad Institute of Massachusetts Institute of Technology and Harvard, Cambridge, Massachusetts; [10]Department of Thoracic Surgery, Samsung Medical Center; [11]Sungkyunkwan University School of Medicine, Seoul, Korea; and [12]Max-Planck Institute, Cologne, Germany

**Note:** Supplementary data for this article are available at Clinical Cancer Research Online (http://clincancerres.aacrjournals.org/).

**Requests for reprints:** Pasi A. Jänne, Lowe Center for Thoracic Oncology, Dana-Farber Cancer Institute, D820A, 44 Binney Street, Boston, MA 02115. Phone: 617-632-6036; Fax: 617-582-7683; E-mail: pjanne@partners.org.

Anaplastic lymphoma kinase (ALK) kinase was originally discovered from chromosomal translocations leading to the production of fusion proteins consisting of the COOH-terminal kinase domain of ALK and the $NH_2$-terminal portions of different genes (1). Translocations of *ALK* have been identified in 40% to 60% of anaplastic lymphomas and in B-cell lymphomas, neuroblastomas, and myofibroblastic tumors (2). *NPM* is the most common fusion partner of *ALK* (80% of translocations), but at least six other fusion partners have been identified (2). In these fusion proteins, the $NH_2$-terminal portion is responsible for protein oligomerization, which leads to constitutive activation of ALK kinase, and results in aberrant activation of downstream signaling targets including Akt, STAT3, and extracellular signal-regulated kinase 1/2 (ERK1/2; ref. 2).

The fusion of the *ALK* gene with echinoderm microtubule-associated protein-like 4 (*EML4*) has recently been detected in 6.7% (5 of 75) of Japanese non-small cell lung cancers (NSCLC; ref. 3). *ALK* and *EML4* are both located in the short arm of chromosome 2 separated by 12 Mb and are oriented in opposite 5′ to 3′ directions. Two different variants of *EML4-ALK* fusion gene have been characterized both involving exons

20 to 29 of *ALK* fused to exons 1 to 13 (variant 1) or exons 1 to 20 (variant 2) of *EML4*. Both variants of the *EML4-ALK* fusion gene were transforming in 3T3 cells and in Ba/F3 models (3).

Inhibitors of ALK kinase have been developed and examined in preclinical models. Proof-of-concept studies using short hairpin RNA knockdown of ALK in *NPM-ALK*-containing models led to growth inhibition and apoptosis and suggested that ALK inhibition may be a potentially effective therapeutic strategy (4). This has lead to the development and testing of small-molecule inhibitors of ALK. Initial studies have been done using less potent ALK inhibitors such as WHI-P154 ($IC_{50}$, ~ 5 μmol/L), pyridones ($IC_{50}$ for staurosporine, 0.15-0.78 μmol/L), or HSP90 inhibitors (5). Subsequently, more potent and specific ALK inhibitors such as diaminopyrimidines or aminopyrimidines have been developed including TAE684 and PF02341066 (6–8). Both of these inhibitors have good bioavailability and inhibit ALK kinase activity and growth of *NPM-ALK*-positive lymphoma cells in the low nanomolar range (6–8). PF02341066 is an inhibitor of both MET and ALK presently in phase I clinical development. TAE684 is not currently under clinical development. Neither agent has been examined previously against *EML4-ALK*.

In the current study, we analyzed the frequency of the *EML4-ALK* fusion gene in NSCLC cell lines and tumors derived from U.S. and Korean NSCLC patients. In addition, we examined the efficacy of an ALK kinase inhibitor, TAE684, in NSCLC cell lines harboring the *EML4-ALK* inversion to determine if this would be a potentially effective therapeutic strategy for NSCLC patients whose tumors contain the *EML4-ALK* inversion (6).

## Materials and Methods

*Cell lines and tumors.* NSCLC (*n* = 81) and mesothelioma (*n* = 2) cell lines were purchased from the American Type Culture Collection or were kind gifts from Drs. John D. Minna and Adi F. Gazdar (University of Texas Southwestern; Supplementary Table S1). DFCI024 and DFCI032 were established at Dana-Farber Cancer Institute from pleural effusions of treatment naive female NSCLC patients. The PC-9, A549, H3122, and H2228 cells were cultured in RPMI 1640 (Sigma) supplemented with 10% fetal bovine serum, 100 units/mL streptomycin, and 1 mmol/L sodium pyruvate. The DFCI032 cells were cultured in ACL-4 medium (Invitrogen) supplemented with 5% fetal bovine serum, 100 units/mL streptomycin, and 1 mmol/L sodium pyruvate.

NSCLC tumors (*n* = 305) were collected from surgical resections from patients with stages I to IIII NSCLC when sufficient material for RNA extraction was available. The majority of the specimens (*n* = 167) were collected at the Samsung Medical Center. Frozen tumor tissues were collected from 809 of 2,442 patients who underwent curative resection for NSCLC from November 1995 to February 2007 at the Samsung Medical Center. One or two pieces from the periphery of the tumor masses, avoiding necrotic regions, were immediately frozen at -80°C until retrieved. The medical records as well as H&E-stained slides of the specimen were reviewed by a single pathologist. Only frozen tumor tissues from adenocarcinoma or squamous cell carcinoma (according to the 2004 WHO histopathologic criteria) were included. Only frozen tumor tissues with a tumor cell content of more than 70% were used for further analysis. In addition, frozen tumor tissues of the following patients were excluded from the study: patients who had received preoperative neoadjuvant treatments, patients with double primary lung cancer, and patients who had undergone incomplete resections or who had not been subjected to mediastinal lymph node dissections. The selected frozen tumor tissues were used for the

microdissection. Briefly, frozen tissues were lightly stained with H&E to improve visualization and the necrotic tumor tissues and intervening normal tissues were removed. Each of the microdissected tumor tissues with a tumor cell content of more than 90% was placed in 1 mL Easy Blue reagent of a commercially available RNA isolation kit (easy-spin Total RNA Extraction Kit; iNtRON Biotechnology) and immediately homogenized by vortexing, and the total RNA was extracted. The quantity and quality of RNA were analyzed using a spectrometer (Nanodrop Technologies) and Agilent 2100 Bioanalyzer (Agilent RNA 6000 Nano Kit; Agilent Technologies), respectively. In the end, 167 frozen tissues with acceptable quality of RNA (RNA integrity number, >7.0) were used for the current studies. All patients provided written informed consent.

The tumors from Caucasian patients (*n* = 138) were collected at the Brigham and Women's Hospital between 1991 and 1997 and have been published previously (9, 10). Frozen samples of resected lung tumors were obtained within 30 min of resection and subdivided into 100 mg samples and snap frozen at -80 C. Each specimen was associated with an immediately adjacent sample embedded for histology in OCT medium and stored at -80 C. Frozen (6 μm) sections of embedded samples stained with H&E was used to confirm the postoperative pathologic diagnosis and to estimate the cellular composition of adjacent samples. All specimens underwent pathologic review by two pathologists. One hundred nine tumors obtained during the same period were excluded because they did not meet one or more of the eligibility criteria. Tissue samples were homogenized in Trizol (Life Technologies) and RNA was extracted and purified by using the RNeasy column purification kit (Qiagen). Denaturing formaldehyde gel electrophoresis followed by Northern blotting using a β-actin probe assessed RNA integrity. Samples were excluded if β-actin was not full-length. All patients provided written informed consent.

Cell line specimens were snap frozen and stored at -80C. RNA was extracted from tumors and cell lines using Trizol (Invitrogen), purified with RNeasy Mini Kit (Qiagen), and used for cDNA synthesis using the QuantiTect reverse transcription kit (Qiagen).

*Exon array studies.* To screen for ALK translocations, we used Affymetrix HuEx-1.0 Exon Array (Affymetrix) data that was generated previously from these cell lines.[13] The HuEx-1.0 array was designed to contain probes mapping to every known and predicted exon in the human genome. We reasoned that translocations in the *ALK* gene would result in disparate levels of expression between exons 5′ and 3′ of the breakpoint, with the expression higher in the 3′ end (kinase domain). After performing array normalization and background correction for all probes, we restricted our analysis to the 104 probes uniquely mapping to the *ALK* gene (Refseq NM_004304). To correct for differences in probe response characteristics across the gene, for every sample, we divided each probe intensity value by the average probe intensity across the other wild-type specimens. For each cell line, we computed the location of the most likely breakpoint as the probe that gives the maximum deviation between average expression of 5′ and 3′ probe subsets. Significance levels for each inferred breakpoint were computed using a simple two-sided *t* test.

*Reverse transcription-PCR and genotyping.* For reverse transcription-PCR analysis of *EML4-ALK*, we used primer sequences (primer set 1) as described in ref. 3. The forward primer is located at exon 13 of *EML4*, whereas the reverse primer is located at exon 20 of *ALK*. To detect other potential *EML4-ALK* fusion products, we designed a second forward primer from exon 3 of *EML4* (5′-taccagtgctgtctcaattgcagg- 3′) while using the same reverse primer as the primer set 1. PCR amplification was done using JumpStart Taq enzyme (Sigma) under the manufacturer's guidelines. The resulting PCR products were analyzed using agarose gel electrophoresis. Genotyping for *KRAS*, *epidermal growth factor receptor* (*EGFR*), *HER2*, *BRAF*, and *PIK3CA* was done using either

---

[13] R.K. Thomas, C.H. Mermel, D. Chiang, and M. Meyerson, unpublished results.
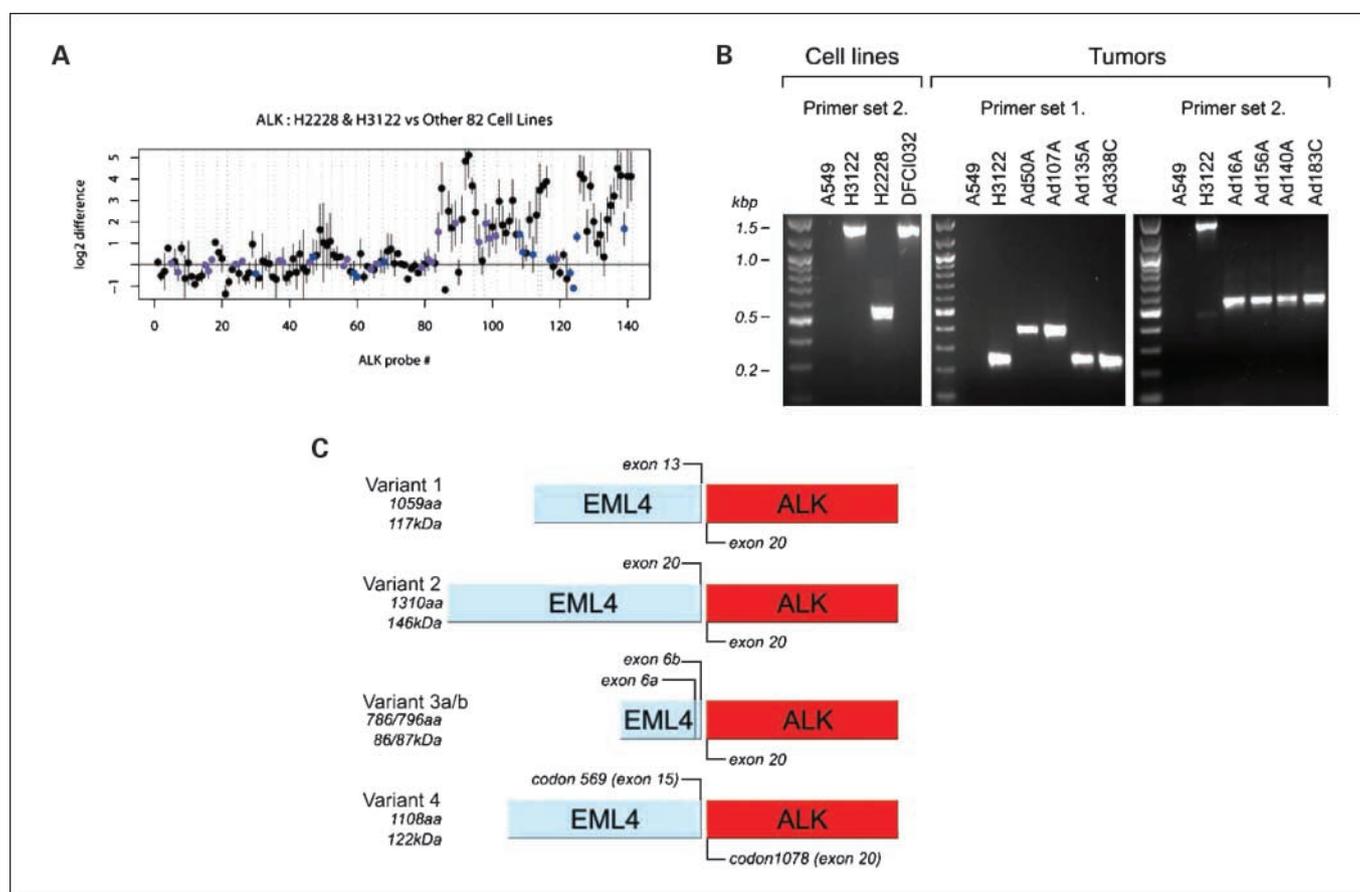
**Fig. 1.** *EML4-ALK* in NSCLC cell lines and tumors. *A,* detection of *ALK* fusion genes in lung cancer cell lines using exon arrays. In the screen of 83 lung cancer cell lines (81 of 83 NSCLC), exon arrays showed that H3122 and H2228 cell lines had significantly higher signal (log₂ difference) for ALK probes 80 to 140 corresponding to exons 20 to 29 of *ALK* compared with other 81 cell lines. Probes were assigned into three categories based on their labeling intensity: nonresponsive probes (*purple*), low-intensity probes (*blue*), and high-intensity probes (*black*). Only high-intensity probes were used in breakpoint detection. *B,* reverse transcription-PCR detection of *EML4-ALK* fusion in NSCLC cell lines and tumors. Primer set 2 amplifies *EML4-ALK* fusion genes from H3122, H2228, and DFCI032 cell lines but not from A549 line. Primer sets 1 and 2 also detected *EML4-ALK* fusion from eight primary NSCLC. H3122, positive control; A549, negative control. *C,* schematic representation of the four different *EML4-ALK* variants in NSCLC.

a reverse transcription-PCR based or a genomic DNA-based SURVEY-OR-WAVE mutation analysis (11) followed by sequencing of the positive specimens or by direct sequencing of the PCR products. Primer sequences and PCR conditions are available upon request.

*Fluorescence* **in situ** *hybridization.* Bacterial artificial chromosomes RP11-667I6 and RP11-100C1 (Children's Hospital Oakland Research Institute) were used as probes for the *EML4* and *ALK* genes, respectively. Bacterial artificial chromosome DNA was labeled with either spectrum red dUTP or spectrum green-11-dUTP by nick translation (Vysis) using manufacturer's recommended conditions. Slides for metaphase fluorescence *in situ* hybridization (FISH) from cell lines were prepared using standard cytogenetic methodologies. Paraffin-embedded slides were prepared as described previously in ref. 11. Probes were hybridized and washed according to standard FISH procedures (12).

*Kinase inhibitors.* TAE684 was synthesized according to published procedures (13). The structure of TAE684 was confirmed using liquid chromatography-mass spectrometry and $^1$H and $^{13}$C nuclear magnetic resonance. The synthesized TAE684 was determined to be 98% pure by $^1$H nuclear magnetic resonance and 99% pure by liquid chromatography-mass spectrometry monitoring at 210 and 254 nm wavelengths (data not shown). CL-387,785 was purchased from Calbiochem. Erlotinib was purchased from the Dana-Farber Cancer Institute pharmacy. All drugs were dissolved in DMSO, stored at -70°C, and diluted in fresh medium before use.

*Cell proliferation and growth assays.* Growth inhibition was assessed by MTS assay as described in ref. 11. NSCLC cells were exposed to drugs alone or in combination for 72 h. All experimental points were set up in 6 to 12 wells and repeated at least three times. The data were graphically displayed using GraphPad Prism version 3.00 for Windows (GraphPad Software).[14] The curves were fitted using a nonlinear regression model with a sigmoidal dose response.

*Antibodies and Western blotting.* Cells were lysed in buffer containing proteinase inhibitors, and proteins separated by gel electrophoresis on 5% to 12% polyacrylamide gels selected depending on the target's molecular weight, transferred to polyvinylidene difluoride membranes, and detected by immunoblotting using an enhanced chemiluminescence system (Perkin-Elmer) as described previously (11). The receptor tyrosine kinase (RTK) array was purchased from R&D Systems and used according to the manufacturer's recommended conditions. Anti-ALK, anti-phospho-ALK (Tyr[1604]), anti-phospho-Akt (Ser[473]), anti-Akt, anti-STAT3, anti-phospho-STAT3 (Tyr[705]), anti-PTEN, and anti–poly(ADP-ribose) polymerase antibodies were obtained from Cell Signaling Technology. Total ERK1/2 and phospho-ERK1/2 (pT185/pY187) antibodies were purchased from Biosource International. The anti-α-tubulin antibody was purchased from Sigma-Aldrich.

---

[14] http://www.graphpad.com
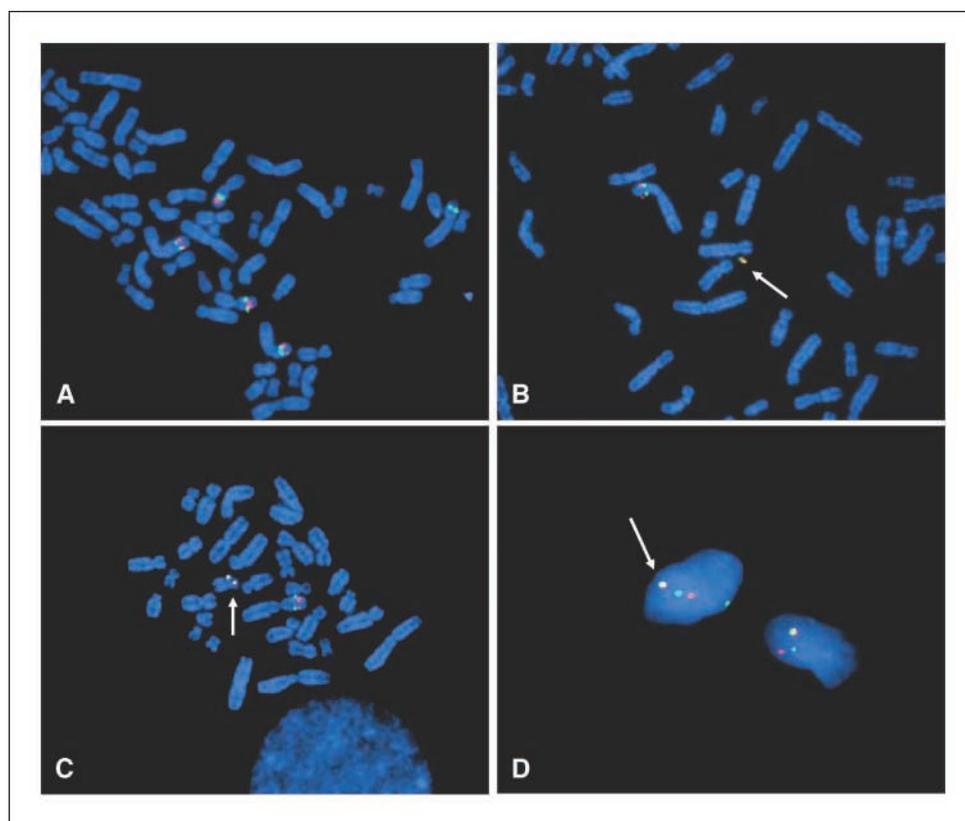
Fig. 2. Detection of *EML4-ALK* using FISH. *A,* PC-9 (*EGFR* del E746.A750) cell line. Signals for *ALK* (*red dot*) and *EML4* (*green dot*) are seen separately. *B,* H2228 cell line. The fusion signal of *EML4-ALK* (*arrow*) is detected in a small extrachromosomal fragment (*yellow*). *C,* DFCI032 cell line. The *EML4-ALK* fusion signal (*yellow; arrow*) is heterozygous. Similar findings were observed for H3122 (data not shown). *D,* interphase FISH for *EML4-ALK* from the formalin-fixed paraffin-embedded tumor specimen obtained from the pleura of the patient whose pleural effusion was used to establish the DFCI032 cell line in *C.* The tumor is heterozygous for the *EML4-ALK* fusion signal (*yellow dot; arrow*).

*Fluorescence-activated cell sorting analysis.* Cells were plated at a density of 0.5 to $2 \times 10^5$ per plate in 10 cm² plates. Drugs were added to the medium after 24 h, and the cells were incubated for another 72 h, after which the cells were analyzed as described previously (14). Percent apoptosis was estimated from the sub-$G_1$ cell fraction.

*Xenograft studies.* Nude mice (*nu/nu*; 6-8 weeks old; Charles River Laboratories) were used for *in vivo* studies and were cared for in accordance with the standards of the Institutional Animal Care and Use Committee under a protocol approved by the Animal Care and Use Committee of the Beth Israel Deaconess Medical Center. Mice were anesthetized using a 2% isofluorane (Baxter) inhalation oxygen mixture. A suspension of $5 \times 10^6$ H3122 lung cancer cells (in 0.2 mL PBS) were inoculated s.c. into the lower right quadrant of the flank of each mouse. Mice were randomized to four treatment groups (*n* = 5 per group) once the mean tumor volume reached 500 to 600 mm³: vehicle (10% 1-methyl-2-pyrrolidinone/90% PEG-300) alone, erlotinib, and 10 and 25 mg/kg/d TAE684 orally (6). Erlotinib was administered at 100 mg/kg/d orally as described previously (11). Tumors were measured twice weekly using calipers, and volume was calculated using the formula: length × width² × 0.52. Mice were monitored daily for body weight and general condition. The experiment was terminated when the mean size of either the treated or control groups reached 2,000 mm³.

## Results

*Identification of* EML4-ALK *fusion genes in NSCLC cell lines.* To rapidly screen our panel of 83 lung cancer cell lines (Supplementary Table S1) for potential *ALK* translocations, we used Affymetrix HuEx-1.0 mRNA exon arrays and focused on 104 unique probes covering the *ALK* gene. We identified two cell lines, H3122 and H2228, which had statistically significant (*P* < 0.001) breakpoints in the *ALK* gene (Fig. 1A;

**Table 1.** Frequency of the *EML4-ALK* fusion gene in NSCLC tumors and its association with clinical, pathologic, and genetic factors

| Clinical, pathologic, and genetic characteristics | EML4-ALK, n (%) | | P* |
|---|---|---|---|
| | + | − | |
| All tumors | 8 (3) | 297 (97) | |
| Ethnicity | | | |
| U.S. cohort | 2 (1) | 136 (99) | NS |
| Korean cohort | 6 (3) | 167 (97) | |
| Gender | | | |
| Male | 3 (2) | 184 (98) | NS |
| Female | 5 (4) | 119 (96) | |
| Smoking (<10 pack-years) | | | |
| Never | 4 (6) | 65 (27) | 0.049 |
| Smoker | 2 (1) | 182 (73) | |
| Age, median (y) | 55.9 | 61.9 | |
| Stage | | | |
| I | 4 (2) | 179 (98) | NS |
| II | 1 (2) | 58 (98) | |
| III | 3 (6) | 47 (94) | |
| IV | 0 (0) | 9 (100) | |
| Histology | | | |
| Adenocarcinoma | 8 (4) | 200 (96) | NS |
| Squamous cell carcinoma | 0 (0) | 88 (100) | |
| Adenosquamous carcinoma | 0 (0) | 9 (100) | |
| Oncogenic mutations | | | |
| EGFR | 1 (1) | 68 (99) | NS |
| KRAS | 0 (0) | 49 (100) | |
| BRAF | 0 (0) | 4 (100) | |

*Fisher's exact test. NS, not statistically significant (*P* > 0.05).

Supplementary Fig. S1). Although our algorithm did not consider the location or direction of the breakpoint, the inferred ALK breakpoints in both samples were very near the conserved exon 20 breakpoint in the ALK gene, and in both samples, the expression was higher in the 3′ than the 5′ ends. Using reverse transcription-PCR, we were able to confirm the presence of the *EML4-ALK* fusion gene product in both H3122 and H2228 but not in any other of the 81 cell lines. In H3122, we detected variant 1 of *EML4-ALK* (Fig. 1B and C). In H2228, we detected a novel variant (named variant 3a hereafter) resulting from a fusion of exon 6 (codons 1-222) of *EML4* with exon 20 (codons 1,058-1,621) of *ALK* (Fig. 1C; Supplementary Fig. S2). A second fusion gene (variant 3b) was also detected from this cell line and contains an additional 33-bp fragment derived from an alternatively spliced exon of

*EML4* (exon 6b; Fig. 1C; Supplementary Fig. S2) and is the predominant form in H2228 (data not shown). This alternatively spliced exon was not detected in any of the other fusion variants. As both H3122 and H2228 cell lines were established from female NSCLC patients with adenocarcinoma and H2228 is from a never-smoker, we screened for the presence of *EML4-ALK* in NSCLC cell lines with these clinical features that we have established at Dana-Farber Cancer Institute. We identified two cell lines, DFCI024 and DFCI032, both derived from chemotherapy naive female never-smokers with adenocarcinoma. Both cell lines are wild-type for *EGFR* and *KRAS*. We detected variant 1 of the *EML4-ALK* fusion gene in the DFCI032 cell line and neither variant in DFCI024 (Fig. 1B). Overall, we detected the *EML4-ALK* fusion gene in 3 of 83 (3.6%) NSCLC cell lines. We further confirmed the presence of

**Fig. 3.** Effect of TAE684 on growth and signaling in *EML4-ALK*-containing NSCLC cell lines. *A,* NSCLC cells were treated with TAE-684 at the indicated concentrations, and viable cells were measured after 72 h of treatment. The percentage of viable cells is shown relative to untreated controls. A549 (*KRAS* G12S), PC-9 (*EGFR* del E746.A750), H2228 (*EML4-ALK* variant 3), H3122 (*EML4-ALK* variant 1), and DFCI032 (*EML4-ALK* variant 1). *B,* fluorescence-activated cell sorting analysis of sub-G$_1$ fraction without treatment (*left column*) and after treatment with 0.1 μmol/L TAE684 for 72 h (*right column*). Significant apoptosis following TAE-684 treatment is only observed in the H3122 cell line. *C,* Western analysis of poly(ADP-ribose) polymerase following treatment with 0.1 μmol/L TAE684 for 72 h. The 89-kDa cleaved poly(ADP-ribose) polymerase products is observed only in the H3122 cell line consistent with the effects of TAE-684 on cell growth in *A. D,* Western analysis following TAE684 treatment in wild-type and *EML4-ALK*-positive NSCLC cell lines. Total and phosphorylated ALK are only detected in *EML4-ALK*-positive cell lines (H3122, H2228, and DFCI032) but not in wild-type control (PC-9). In H3122 and DFCI032 cell lines, ALK-positive band migrates at ~120 kDa corresponding to predicted molecular weight (117 kDa) of the variant 1 (*arrow 1*), whereas in H2228 the band migrates at ~90 kDa, which also corresponds to the predicted molecular weight (90/91 kDa) of the variant 3 (*arrow 3*). ALK phosphorylation is completely inhibited following 0.1 μmol/L TAE684 treatment (6 h) in all the cell lines. Phosphorylation of Akt, STAT3, and ERK1/2 decreases in H3122 and H2228 cell lines with TAE684 but remain unchanged in DFCI032 and PC-9 lines. All the cell lines show presence of PTEN. α-Tubulin is used as a loading control.
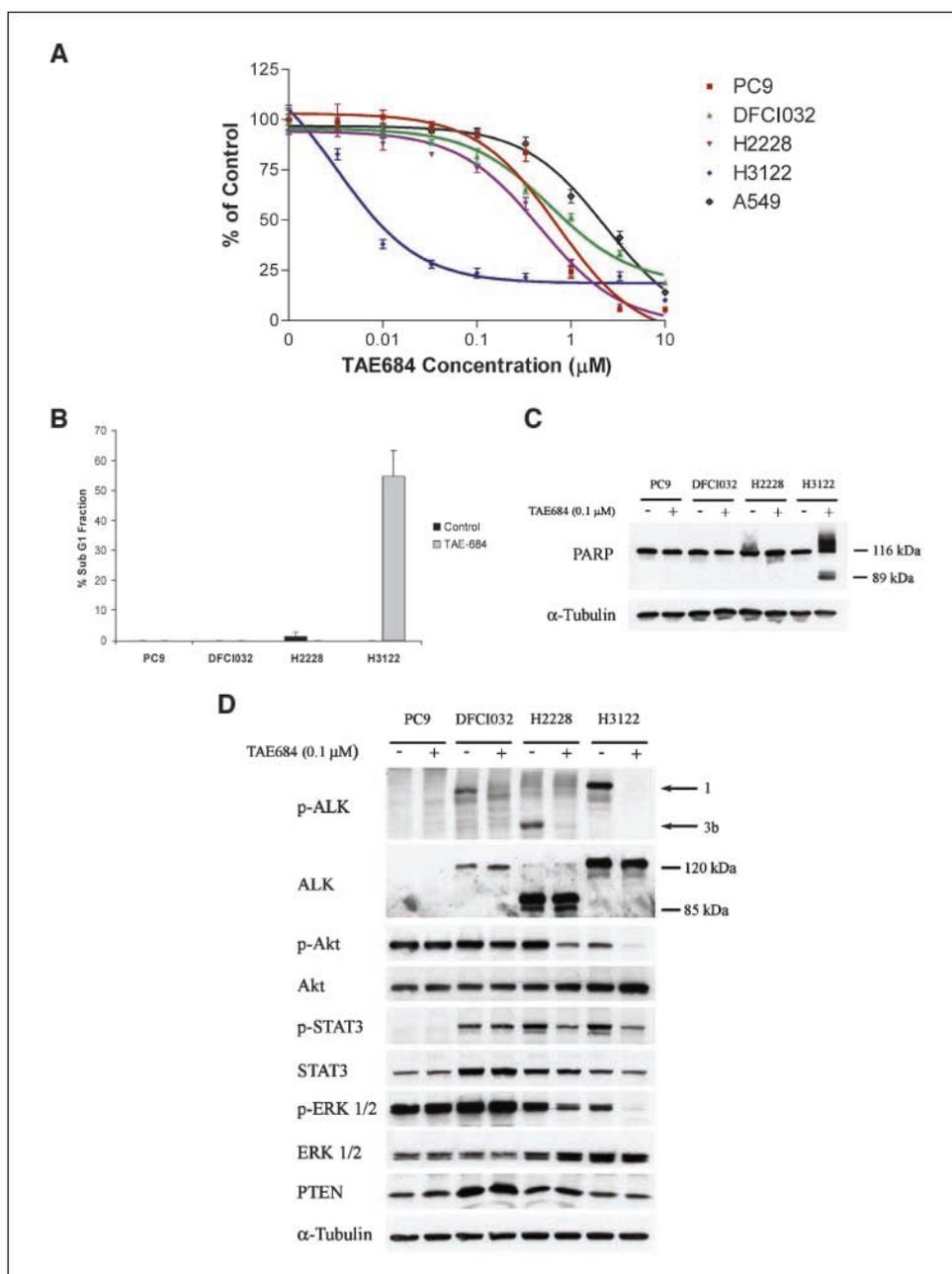
the *EML4-ALK* inversion using FISH (Supplementary Fig. S3) in these three cell lines (Fig. 2A-C). In addition, we confirmed the presence of the *EML4-ALK* fusion in the original tumor specimen that gave rise to the DFCI032 cell line using interphase FISH (Fig. 2D).

**EML4-ALK** *fusion gene is detected in both Caucasian and Asian NSCLC.* We screened NSCLC (n = 305) from patients of U.S. (n = 138) and Korean (n = 167) origin for the *EML4-ALK* fusion gene and detected its presence in 8 of 305 (3%) NSCLC (Table 1). Four tumors contained variant 3 (both variants 3a and 3b, with 3b being predominant), two contained variant 1, and two contained a novel variant (named variant 4 hereafter; Fig. 1B and C). In variant 4, exon 15 of *EML4* is fused with exon 20 of *ALK* (*EML4* codons 1-569 to 1,078-1,621 of ALK; Fig. 1C; Supplementary Fig. S2). Six of the *EML4-ALK*-containing tumors (6 of 167; 3.6%) were from Korean patients, whereas 2 of 138 (1.5%) were detected in NSCLC from U.S. patients. The frequency of *EML4-ALK* was higher in females (4%) versus males (2%). All eight of the *EML4-ALK*-containing tumors were adenocarcinomas. Furthermore, the fusion gene was detected significantly ($P = 0.049$; Table 1) more frequently in patients (6%; 4 of 69) with limited smoking history (<10 pack-years) compared with tumors from smokers (1%; 2 of 184). The tumor from one of the patients had a concurrent *EGFR* kinase domain mutation (del E746_A750) with the *EML4-ALK* fusion gene. None of the eight tumors contained a concurrent *KRAS* or *BRAF* mutation (data not shown).

*Inhibition of ALK kinase activity in* **EML4-ALK** *fusion gene in vitro and in vivo.* To determine whether ALK kinase inhibitors may be therapeutically effective in *EML4-ALK*-containing NSCLC, we evaluated TAE684, a highly potent ALK kinase inhibitor (6). We found that TAE684 significantly inhibited the growth of only the H3122 cell line, whereas the other two *EML4-ALK*-containing cell lines, H2228 and DFCI032, were as resistant (IC$_{50}$, 1-10 μmol/L) to the inhibitor as those containing an *EGFR* mutation (PC-9; del E746_A750) or a *KRAS* mutation (A549; G12S; Fig. 3A). It should be noted that the IC$_{50}$ for the H3122 cells is 10 nmol/L and that TAE684 exhibits its maximal effects in this responsive cell line at 100 nmol/L (Fig. 3A). At these low concentrations, TAE684 is highly selective for ALK; therefore, the observed response is not likely to be due to off-target effects (6). Conversely, the effects on the *EGFR* mutant PC-9 and *KRAS* mutant A549 cells, which are not ALK dependent for their growth, at concentrations >1 μmol/L are likely to be due to off-target effects; thus, we used 100 nmol/L TAE684 for subsequent studies. TAE684 (100 nmol/L) treatment led to significant apoptosis only in the H3122 cell line as detected by fluorescence-activated cell sorting (Fig. 3B) or by Western blotting for cleaved poly(ADP-ribose) polymerase (Fig. 3C). No growth arrest or apoptosis was observed in the other cell lines following TAE684 treatment.

To determine why the growth of only one of three of the *EML4-ALK*-containing cell lines was inhibited by TAE684, we examined its effects on phosphorylation of ALK and downstream signaling proteins (Fig. 3D). Following 100 nmol/L TAE684 treatment, complete inhibition of phosphorylated ALK was observed in all three of the *EML4-ALK*-positive cell lines (Fig. 3D). However, this was accompanied by substantial inhibition of Akt as well as ERK1/2 phosphorylation only in the H3122 cell line consistent with the effects on cell growth and apoptosis in this cell line (Fig. 3A-C). In contrast to Akt and

ERK1/2, there was only a minimal decrease in STAT3 phosphorylation following TAE684 treatment in the H3122 cell line (Fig. 3D). In the H2228 cell line, there was some but not complete inhibition of Akt and ERK1/2 phosphorylation, whereas these were unchanged in the DFCI032 cell line (Fig. 3D).

We also examined the effects of TAE684 treatment on H3122 *in vivo* using a xenograft model. We compared the effects of TAE684 with the EGFR kinase inhibitor erlotinib, which did not inhibit the growth of H3122 cells *in vitro* (IC$_{50}$ >10 μmol/L; data not shown). We used erlotinib because we detected *EML4-ALK* significantly more frequently in never or former light cigarette smokers with NSCLC (Table 1) and because erlotinib is frequently used in clinical trials in this same patient population (11, 15). Thus, we wished to determine the efficacy of erlotinib in *EML4-ALK*-containing NSCLC. We also explored the dosing of TAE684 by examining two different doses in the xenograft studies. As can be seen in Fig. 4, both doses of TAE684 effectively inhibited the growth of H3122 xenografts. Both vehicle-treated and erlotinib-treated mice were all sacrificed following 2 weeks of treatment due to rapid tumor growth. These are consistent with the effects of erlotinib *in vitro* (data not shown). The higher dose of TAE-684 (25 mg/kg/d) more effectively inhibited tumor growth than the lower (10 mg/kg/d) dose (Fig. 4). The 25 mg/kg/d dose was associated with an initial shrinkage of established tumors followed by stabilization. All mice were sacrificed at day 53 of treatment.

*Coactivation of ERBB family members in an* **EML4-ALK**-*containing NSCLC.* In the DFCI032 cell line, which contains the exact same *EML4-ALK* variant as H3122 (Fig. 1B), TAE684 completely inhibited ALK phosphorylation, but this was not accompanied by inhibition of growth or changes in phosphorylation of Akt or ERK1/2 (Fig. 3A and D). DFCI032 is not a heterogeneous cell line as by FISH we were able to detect *EML4-ALK* in 100% of the cells (data not shown). We also did not detect a concurrent mutation in the known oncogenes (*EGFR*, *KRAS*, *BRAF*, *HER2*, or *PIK3CA*) commonly mutated in NSCLC
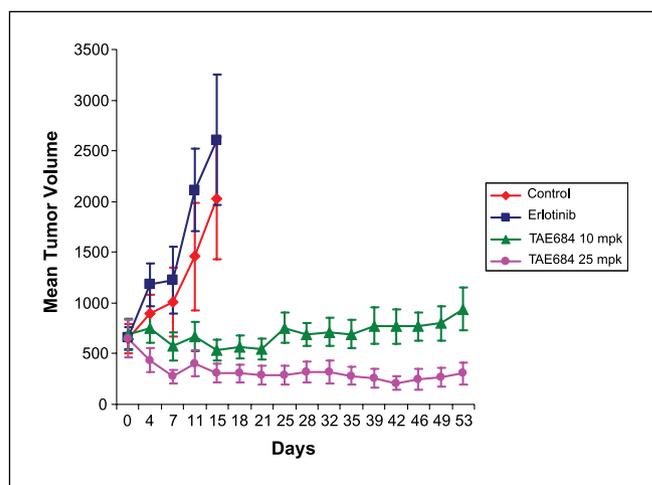


**Fig. 4.** TAE-684 effectively inhibits the growth of H3122 *in vivo*. Xenografts on H3122 in *nu/nu* mice were generated as described in Materials and Methods. Erlotinib and TAE-684 treatments were administered by oral gavage and tumors were measured three times weekly. The control and erlotinib-treated mice reached a median tumor size of 2,000 mm$^3$ by 15 d of treatment and were sacrificed. In contrast, the median tumor size of mice treated with TAE684 at either 10 or 25 mg/kg/d did not reach 2,000 mm$^3$ even after 53 days of treatment.

in the DFCI032 cell line (data not shown). Recent studies have shown that in some cancers multiple RTK can be coactivated (11, 16). Inhibition of only one of the coactivated kinases is insufficient to result in inhibition of growth or Akt phosphorylation (11, 16). To determine whether DFCI032 contained other activated kinases, we performed a screen using a phospho-RTK array comprising 42 RTK. As can be seen in Fig. 5A, the two most intense signals detected in this array were for phosphorylated EGFR and ERBB2. Low-level activation of other RTK were also observed, but the signals were substantially weaker than for EGFR and ERBB2 (Fig. 5A). ALK is not present on this array (data not shown). We next examined the effects of CL-387,785 (1 μmol/L), an irreversible EGFR and ERBB2 inhibitor, alone or in combination with TAE684 (100 nmol/L) in the DFCI032 cell line. The combination of CL,387,785 and TAE684, but not either agent alone, significantly inhibited the growth of DFCI032 cells and was associated with significant apoptosis (Fig. 5C and D). Furthermore, only the combination of TAE684 and CL-387,785 was associated inhibition of Akt and ERK1/2 phosphorylation (Fig. 5D). We also examined the combination of the EGFR inhibitor gefitinib (1 μmol/L) and TAE684 (100 nmol/L) and observed no effect on growth of DFCI032 cells (data not shown). These findings suggest that inhibition of both EGFR and ERBB2 along with ALK is necessary to effectively inhibit growth and induce apoptosis in the DFCI032 cell line.

## Discussion

The use of molecular targeted therapy in genetically defined subsets of cancer patients is emerging as an effective therapeutic strategy for many cancers (17–19). In lung cancer, for example, 10% to 30% of NSCLC contain activating mutations in the EGFR kinase domain and 60% to 80% of the patients with EGFR mutations obtain dramatic radiographic responses following treatment with the EGFR kinase inhibitors gefitinib or erlotinib (11, 19). Similarly, EGFR mutant NSCLC cell lines are exquisitely sensitive to gefitinib *in vitro* compared with EGFR wild-type cell lines and only EGFR mutant NSCLC cell lines undergo apoptosis following gefitinib treatment (14, 20, 21). Thus, it remains critical to identify subsets of lung cancer patients and to develop effective therapeutic strategies for such patients. As lung cancer is a very common cancer, the identification of even small subsets of lung cancer patients harboring specific genetic alterations will translate into a large cohort of patients.

In the present study, we characterized the frequency of the EML4-ALK inversion in NSCLC cell lines and primary tumors from NSCLC patients of different ethnic backgrounds. We detected the EML4-ALK fusion gene in 3% of NSCLC specimens, numerically more frequently from Korean than U.S. NSCLC patients, adenocarcinomas, and in patients with limited cigarette smoke exposure. Our study is the first example addressing the frequency of EML4-ALK in Caucasian NSCLC patients. Despite the low frequency of EML4-ALK in NSCLC, this represents more patients (~5,000 annually in United States) than those diagnosed with anaplastic large cell lymphoma where ALK translocations have been detected previously (22, 23). We detected EML4-ALK significantly more frequently (Table 1) from NSCLC patients who were either never or former light (≤10 pack-years) cigarette smokers. This

same clinical feature has also been shown to predict for presence of EGFR mutations (24). Thus, it is possible that NSCLC arising in never/former light smokers are genetically and biologically different from those arising in smokers and more likely to contain activated oncogenes. We detected four different variants of EML4-ALK (Fig. 1) containing virtually identical portions of ALK, comprising the entire kinase domain, with varying portions of EML4. These variants are similar to previously described translocations of ALK with other genes; all of which contain the cytoplasmic portion and entire tyrosine kinase domain of ALK (22). We also developed a FISH assay, which can be used to detect the EML4-ALK inversion from routine paraffin-embedded lung cancer clinical specimens. This will facilitate the identification of appropriate NSCLC patients for clinical studies of ALK kinase inhibitors.

One of the three cell lines with the EML4-ALK translocation (H3122) was also found to be exquisitely sensitive to TAE684 *in vitro* and *in vivo* (Figs. 3A and 4). In addition, TAE684 treatment was associated with significant apoptosis and downregulation of Akt and ERK1/2 signaling (Fig. 3B-D). These findings suggest the phenomenon of oncogene addiction where ALK kinase solely controls the critical survival signaling pathways in this cell line (25). ALK inhibition leads to inhibition of all of these signaling pathways and subsequently to apoptosis. This is analogous to gefitinib treatment of EGFR mutant NSCLC and suggests that ALK kinase inhibitors alone may be effective therapies at least for some patients whose tumors contain EML4-ALK (14, 26). Interestingly, TAE-684 led to only a minimal decrease in STAT3 phosphorylation in H3122 despite causing apoptosis in this cell line (Fig. 3D). STAT3 has been shown to be critical to NPM-ALK-mediated lymphomagenesis and inhibition of STAT3 alone using a dominant-negative STAT3 is sufficient to induce apoptosis (27, 28). There may be signaling differences between NPM-ALK-containing and EML4-ALK-containing tumors or this may reflect differences between NSCLC and anaplastic large cell lymphoma. Further studies will be are necessary to determine the significance of STAT3 signaling in EML4-ALK-containing NSCLC.

Only one of three NSCLC cell lines (H3122) with EML4-ALK was sensitive to the ALK kinase inhibitor alone. The two other EML4-ALK-containing cell lines were either resistant to TAE684 alone (H2228) or required concomitant inhibition of EGFR and ERBB2 (DFCI032). These findings are quite different from EGFR mutant NSCLC cell lines where the majority are exquisitely sensitive to gefitinib or erlotinib *in vitro* and the growth inhibition is accompanied by apoptosis and significant inhibition of EGFR, ERK1/2, and Akt phosphorylation (14, 29, 30). These differences may be clinically significant and highlight the possibility that ALK inhibitors alone may only be effective in a subset of NSCLC patients with the EML4-ALK inversion. Our studies of DFCI032 suggest that it contains coactivation of both EGFR and ERBB2 as concomitant inhibition of ALK, EGFR, and ERBB2 is required to significantly effect growth, induce apoptosis, and inhibit Akt and ERK1/2 phosphorylation (Fig. 5). Thus, our findings provide one potential mechanism, activation of other RTK, by which resistance could emerge in NSCLC patients being treated with ALK inhibitors. In addition, these data suggest that, in some EML4-ALK-containing NSCLC, a combination therapeutic strategy may be necessary. Our findings are analogous to those

found in subsets of glioblastoma multiforme and in *MET*-amplified gefitinib-resistant lung cancers where multiple kinases are coactivated and inhibition of one kinase alone is not sufficient to effect growth or lead to down-regulation of Akt

(11, 16). In H2228, we did not detect coactivation of another kinase (data not shown). The lack of efficacy of TAE684 in our study in H2228 is similar with recent studies using an ALK-specific small interfering RNA, which also did not inhibit the
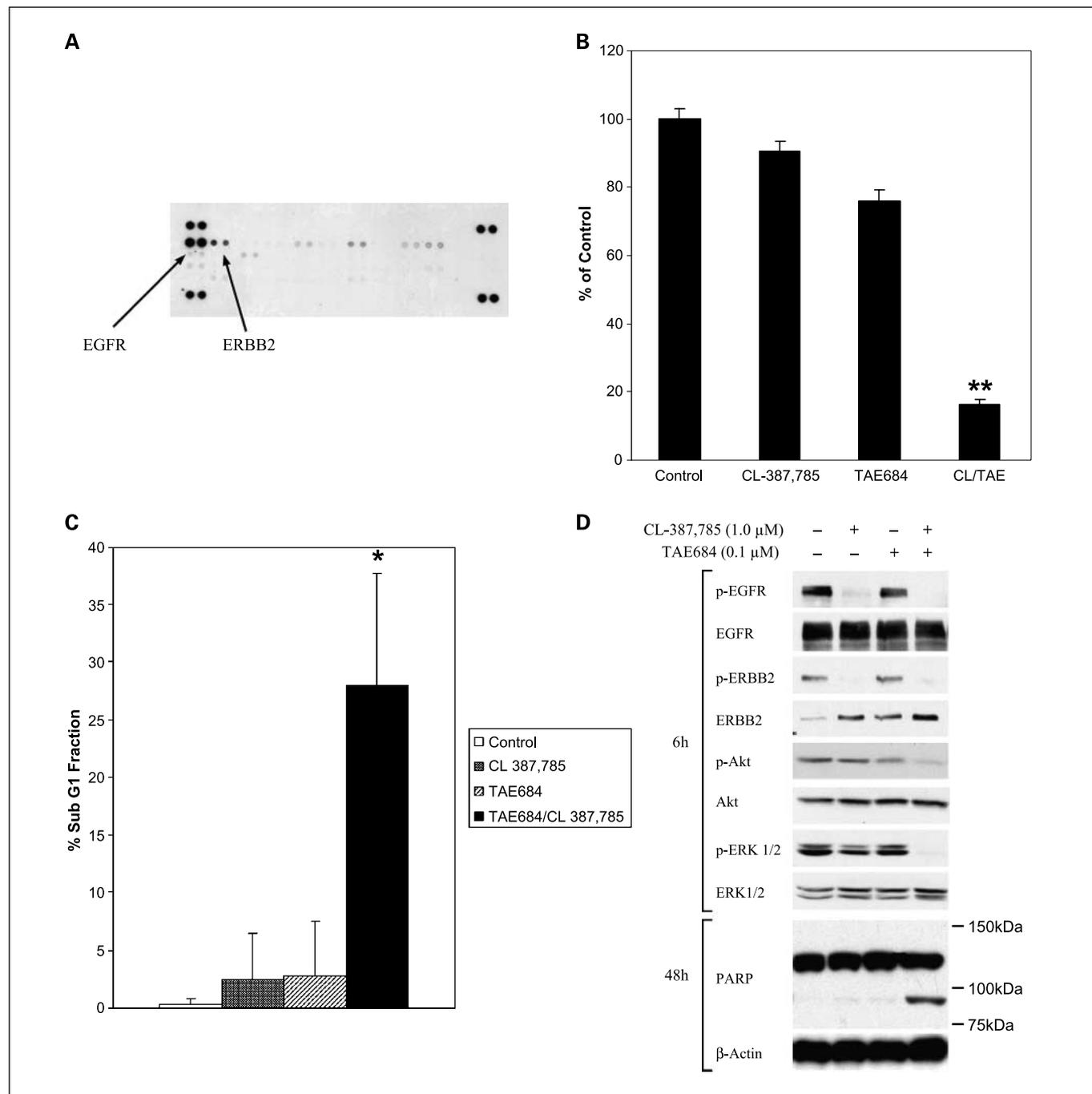
**Fig. 5.** Coactivation of EGFR and ERBB2 in DFCI032 cell line. *A,* a phospho-RTK array reveals that the DFCI032 cells contain strong activation of both EGFR and ERBB2. Cells were grown in medium and the cell lysates were hybridized to a phospho-RTK array. In the array, each RTK is spotted in duplicate. Hybridization signals at the corners serve as controls. *B,* combination of TAE684 and CL-387,785 effectively inhibits growth of DFCI032 cells. DFCI032 cells were treated with either CL-387,785 (1 μmol/L) alone, TAE684 (100 nmol/L) alone, or the two in combination for 72 h. Growth was assayed by MTS (see Materials and Methods). The combination of TAE684 and CL-387,785 led to significant inhibition of growth compared with untreated ($P < 0.001$, paired $t$ test) or treatment with either agent alone ($P < 0.001$, paired $t$ test for both comparisons, respectively). **, $P < 0.001$. *C,* combination of CL-387,785 and TAE-684 leads to significant apoptosis. Cells were treated as in *B* and apoptosis was estimated from sub-G$_1$ fraction using fluorescence-activated cell sorting (Materials and Methods). The combination of CL-387,785 and TAE-684 led to significant increase in apoptosis compared with untreated ($P < 0.05$, paired $t$ test) or treatment with either agent alone ($P < 0.05$, paired $t$ test for both comparisons, respectively). *, $P < 0.05$. *D,* combination of CL-387,785 and TAE-684 leads to inhibition of Akt and ERK1/2 phosphorylation. Cells were treated as in *B* for 6 or 48 h. Cells were lysed and the indicated proteins were detected by immunoblotting. Only the combination of CL-387,785 and TAE-684 leads to significant down-regulation of Akt and ERK1/2 signaling and to apoptosis as measured by appearance of cleaved (89 kDa) poly(ADP-ribose) polymerase fragment.

growth of H2228 cells (31). It will continue to be important to study H2228 and other *EML4-ALK*-containing tumors to determine whether an ALK inhibitor alone or in combination with other kinase inhibitors will be necessary for growth inhibition and apoptosis.

## Disclosure of Potential Conflicts of Interest

J. Engelman (member of Hoffman-LaRoche advisory board) and N. Gray (former Novartis employee) received research grant from Novartis and M. Meyerson received a research grant from Novartis and consults for Novartis. The other authors disclosed no potential conflicts of interest.

## References

**1.** Morris SW, Kirstein MN, Valentine MB, et al. Fusion of a kinase gene, ALK, to a nucleolar protein gene, NPM, in non-Hodgkin's lymphoma. Science 1994;263: 1281–4.

**2.** Amin HM, Lai R. Pathobiology of ALK+ anaplastic large-cell lymphoma. Blood 2007;110:2259–67.

**3.** Soda M, Choi YL, Enomoto M, et al. Identification of the transforming EML4-ALK fusion gene in non-small-cell lung cancer. Nature 2007;448:561–6.

**4.** Piva R, Chiarle R, Manazza AD, et al. Ablation of oncogenic ALK is a viable therapeutic approach for anaplastic large-cell lymphomas. Blood 2006;107: 689–97.

**5.** Li R, Morris SW. Development of anaplastic lymphoma kinase (ALK) small-molecule inhibitors for cancer therapy. Med Res Rev 2008;28:372–412.

**6.** Galkin AV, Melnick JS, Kim S, et al. Identification of NVP-TAE684, a potent, selective, and efficacious inhibitor of NPM-ALK. Proc Natl Acad Sci U S A 2007; 104:270–5.

**7.** Zou HY, Li Q, Lee JH, et al. An orally available small-molecule inhibitor of c-Met, PF-2341066, exhibits cytoreductive antitumor efficacy through antiproliferative and antiangiogenic mechanisms. Cancer Res 2007;67:4408–17.

**8.** Christensen JG, Zou HY, Arango ME, et al. Cytoreductive antitumor activity of PF-2341066, a novel inhibitor of anaplastic lymphoma kinase and c-Met, in experimental models of anaplastic large-cell lymphoma. Mol Cancer Ther 2007;6:3314–22.

**9.** Bhattacharjee A, Richards WG, Staunton J, et al. Classification of human lung carcinomas by mRNA expression profiling reveals distinct adenocarcinoma subclasses. Proc Natl Acad Sci U S A 2001;98: 13790–5.

**10.** Hayes DN, Monti S, Parmigiani G, et al. Gene expression profiling reveals reproducible human lung adenocarcinoma subtypes in multiple independent patient cohorts. J Clin Oncol 2006;24:5079–90.

**11.** Engelman JA, Zejnullahu K, Gale CM, et al. PF00299804, an irreversible pan-ERBB inhibitor, is effective in lung cancer models with EGFR and ERBB2 mutations that are resistant to gefitinib. Cancer Res 2007;67:11924–32.

**12.** Lee C, Critcher R, Zhang JG, Mills W, Farr CJ. Distribution of gamma satellite DNA on the human X and Y chromosomes suggests that it is not required for mitotic centromere function. Chromosoma 2000;109: 381–9.

**13.** Garcia-Echeverria C, Kanazawa T, Kawahara E, et al. Preparation of 2,4-pyrimidinediamines useful in the treatment of neoplastic diseases, inflammatory and immune system disorders. U.S. Patent WO2005016894; 2005.

**14.** Tracy S, Mukohara T, Hansen M, et al. Gefitinib induces apoptosis in the EGFRL858R non-small-cell lung cancer cell line H3255. Cancer Res 2004;64:7241–4.

**15.** Tsao MS, Sakurada A, Cutz JC, et al. Erlotinib in lung cancer—molecular and clinical predictors of outcome. N Engl J Med 2005;353:133–44.

**16.** Stommel JM, Kimmelman AC, Ying H, et al. Coactivation of receptor tyrosine kinases affects the response of tumor cells to targeted therapies. Science 2007;318:287–90.

**17.** Druker BJ, Talpaz M, Resta DJ, et al. Efficacy and safety of a specific inhibitor of the BCR-ABL tyrosine kinase in chronic myeloid leukemia. N Engl J Med 2001;344:1031–7.

**18.** Demetri GD, von Mehren M, Blanke CD, et al. Efficacy and safety of imatinib mesylate in advanced gastrointestinal stromal tumors. N Engl J Med 2002;347: 472–80.

**19.** Inoue A, Suzuki T, Fukuhara T, et al. Prospective phase II study of gefitinib for chemotherapy-naive patients with advanced non-small-cell lung cancer with epidermal growth factor receptor gene mutations. J Clin Oncol 2006;24:3340–6.

**20.** Paez JG, Janne PA, Lee JC, et al. EGFR mutations in lung cancer: correlation with clinical response to gefitinib therapy. Science 2004;304:1497–500.

**21.** Mukohara T, Civiello G, Johnson BE, Janne PA. Therapeutic targeting of multiple signaling pathways in malignant pleural mesothelioma. Oncology 2005; 68:500–10.

**22.** Pulford K, Morris SW, Turturro F. Anaplastic lymphoma kinase proteins in growth control and cancer. J Cell Physiol 2004;199:330–58.

**23.** Jemal A, Siegel R, Ward E, et al. Cancer statistics, 2007. CA Cancer J Clin 2007;57:43–66.

**24.** Pham D, Kris MG, Riely GJ, et al. Use of cigarette-smoking history to estimate the likelihood of mutations in epidermal growth factor receptor gene exons 19 and 21 in lung adenocarcinomas. J Clin Oncol 2006;24:1700–4.

**25.** Weinstein IB. Cancer. Addiction to oncogenes—the Achilles heal of cancer. Science 2002;297:63–4.

**26.** Sordella R, Bell DW, Haber DA, Settleman J. Gefitinib-sensitizing EGFR mutations in lung cancer activate anti-apoptotic pathways. Science 2004; 305:1163–7.

**27.** Chiarle R, Simmons WJ, Cai H, et al. Stat3 is required for ALK-mediated lymphomagenesis and provides a possible therapeutic target. Nat Med 2005;11: 623–9.

**28.** Amin HM, McDonnell TJ, Ma Y, et al. Selective inhibition of STAT3 induces apoptosis and G(1) cell cycle arrest in ALK-positive anaplastic large cell lymphoma. Oncogene 2004;23:5426–34.

**29.** Mukohara T, Engelman JA, Hanna NH, et al. Differential effects of gefitinib and cetuximab on non-small-cell lung cancers bearing epidermal growth factor receptor mutations. J Natl Cancer Inst 2005; 97:1185–94.

**30.** Amann J, Kalyankrishna S, Massion PP, et al. Aberrant epidermal growth factor receptor signaling and enhanced sensitivity to EGFR inhibitors in lung cancer. Cancer Res 2005;65:226–35.

**31.** Rikova K, Guo A, Zeng Q, et al. Global survey of phosphotyrosine signaling identifies oncogenic kinases in lung cancer. Cell 2007;131:1190–203.